

## Research Article

# The Influence of High-Temperature Nitrogen Plasma-Based Ion Implantation on Niobium Creep Behavior

Aline Capella de Oliveira <sup>1</sup>, Joares Lidovino dos Reis,<sup>1</sup> Rogerio Moraes Oliveira,<sup>2</sup> and Danieli Aparecida Pereira Reis<sup>1</sup>

<sup>1</sup>Federal University of Sao Paulo, Rua Talim 330, São José dos Campos, SP 12231-280, Brazil

<sup>2</sup>National Institute for Space Research, Avenida dos Astronautas 1758, São José dos Campos, SP 12227-010, Brazil

Correspondence should be addressed to Aline Capella de Oliveira; [aline.capella@unifesp.br](mailto:aline.capella@unifesp.br)

Received 30 April 2020; Revised 30 June 2020; Accepted 14 July 2020; Published 12 August 2020

Academic Editor: Sakar Mohan

Copyright © 2020 Aline Capella de Oliveira et al. This is an open access article distributed under the Creative Commons Attribution License, which permits unrestricted use, distribution, and reproduction in any medium, provided the original work is properly cited.

Niobium has been considered for applications in the aerospace sector, but its use at high temperatures is restricted, due to the great affinity of refractory metals with oxygen, which results in the formation of oxide layers and a decrease in their mechanical resistances. In the present work, Nb samples were submitted to High-Temperature Nitrogen Plasma-Based Ion Implantation (HT-NPBII). The process runs at a working pressure between 3 and 4 mbar and negative high voltage pulses of 7 kV/30  $\mu$ s/300 Hz were applied to samples heated to 1000°C, at treatment times of 1 h, 4 h, and 8 h, respectively. Microstructural and mechanical characterizations of the treated samples revealed the formation of a layer of Nb<sub>2</sub>N, with 3.0  $\mu$ m thickness and increase in the surface hardness from 225 HV for the untreated material up to about 2498 HV, for samples treated during 8 h. Creep tests were performed at 500°C and with loads varying from 25 to 40 MPa. Results indicated a decrease in the secondary creep rate for treated specimens when compared to the untreated ones. This behavior can be attributed to the formation of a nitride layer on the surface of Nb that acts as barrier to avoid the oxygen diffusion into the material under high temperature conditions.

## 1. Introduction

Niobium has been widely employed as an alloying element due to its outstanding properties such as good corrosion resistance, high melting point, high thermal conductivity, and high linear coefficient of thermal expansion [1] even though the pure metal presents low resistance to oxidation, especially at elevated temperatures, leading to its embrittlement. Thus, improving the surface properties of niobium is necessary for its application at high temperatures in an oxidative environment [2]. The effectiveness of HT-NPBII for the treatment of metal alloys and refractory metals was reported in [3–5]. Details about this process can be found in [6]. The absorption of nitrogen under the influence of high temperature is magnified, leading to the formation of thick nitrated layers. In the case of Nb, the formation of nitrides in the upper layers of the metal can significantly improve its

mechanical and tribological properties [4] as well as its oxidation resistance [3]. In fact, implantation of nitrogen into niobium at 1000°C and 1250°C via HT-NPBII led to the appearance of different phases of niobium nitrides (NbN, Nb<sub>2</sub>N, and Nb<sub>4</sub>N<sub>3</sub>), which resulted in significant increase in hardness and wear reduction, besides causing a retard in the oxidation of the metal by about 130°C [7–10].

The substrate heating during treatments can also promote the increase in the metal grain size [11] which keeps a close relation with its creep behavior. Several studies have reported the influence of the creep response of the treated material under this condition [12–16]. The aim of this paper is to evaluate the creep behavior of niobium treated by HT-NPBII. Microstructural changes caused by the surface treatment were evaluated, followed by mechanical tests performed to investigate the material creep properties. This is an important issue for the application of niobium in

aerospace components submitted to harsh environments under high temperatures.

## 2. Experimental Details

Niobium disks with diameters of 13 mm and thicknesses of 5.0 mm were used as samples for HT-NPBII. They were grinded with abrasive paper (SiC grits of 240, 400, 600, and 1200, sequentially), polished to a mirror-like finish and then cleaned with ethanol in an ultrasonic bath equipment to remove residual contaminants.

HT-NPBII was performed at nitrogen working pressures ranging from 3-4 mbar, by applying high negative voltage pulses to the samples (7 kV/30  $\mu$ s/300 Hz), for 1, 4, and 8 h, respectively. The heating of the substrates is performed by the own ion implantation during pulse on time and mostly by electrons produced by a low work-function thermionic oxide cathode during pulse off time [6]. A positive DC voltage between 50 and 100 V is applied to the substrates to attract electrons when the HV pulse is off. The experimental apparatus used to perform the HT-NPBII can be seen in Figure 1. In order to make this heating process more efficient, instead of using a sample holder which would drain excessive current from the HV power supply, the samples were supported by a thin 0.25 mm diameter tungsten rod. The remaining electrical contact parts, from the wire to the feedthrough in the chamber wall, were isolated from plasma by alumina tubes. Thus, it was possible to concentrate most of the applied power to the samples only. All samples were treated at temperature of 1200°C.

Metallographic analysis was performed on the transverse sections of the samples by optical microscopy (OM, Zeiss, Axioscope A1) and by scanning electron microscopy (SEM, Inspect S50, FEI Company). For these measurements, the samples were grinded with abrasive paper (SiC grits of 240, 400, 600, and 1200, sequentially), polished to a mirror-like finish and chemically etched using Villela's reagent (5 mL HCl + 2 g Picric acid + 100 mL ethyl alcohol). Samples were then cleaned with ethanol in an ultrasonic bath equipment.

The phase composition of the treat metal was analyzed by X-ray diffraction (XRD) (Rigaku diffractometer, Ultima IV in a standard theta-2theta Bragg-Brentano configuration with Cu  $K\alpha$  radiation). The phase identification was performed by analysis of diffraction patterns by the PANalytical High Score software. The surface nanohardness measurements (nanodurometer, MHT3 Anton Paar Testers) were performed in different regions of the samples, considering the modified layer and the base material.

Constant load creep tests, performed according to ASTM E139 standard [17], were carried out in air, with stress levels of 25, 30, 35, and 40 MPa at a constant temperature of 500°C. The specimens were machined according to ASTM E139 standard. For clarity, the dimensions of the specimen are shown in Figure 2. After test, fractographic analysis was carried out in order to identify the operating fracture mechanism. This analysis consists of the observation of one of the fractured surfaces of each broken specimen by means of scanning electron microscopy (SEM).

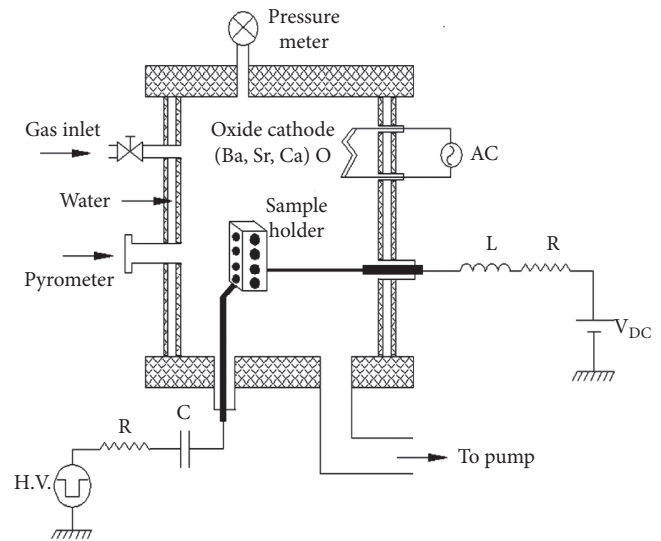


FIGURE 1: Schematic drawing of HT-NPBII apparatus.

## 3. Results and Discussion

X-ray diffraction (XRD) patterns of the samples treated by HT-NPBII confirm the presence of several  $Nb_2N$  phases (JCPDS 01-075-0952), as shown in Figure 3, for all the treatment times. However, it is noticed that the duration of the treatment does not significantly influence on the formation of nitride phases, since the number of peaks in the diffractogram is the same, as well as similar intensities were detected.

On the other hand, distinct treatment times lead to the achievement of modified layers with distinct thickness, as can be seen by the cross-sectional views in Figures 4(a)–4(c), for samples implanted during 1 h, 4 h, and 8 h, respectively. In fact, for the shortest treatment time, the measured thickness was about 1.5  $\mu$ m, against 3.0  $\mu$ m for the sample treated during 4 h. The extension of the duration of the process up to 8 h did not cause a significant variation of the respective thickness, probably due to the attainment of the terminal solubility of niobium for the absorption of nitrogen.

Oliveira et al. [5] reported a nitrogen peak concentration reaching about 45 at.% in the very near surface of implanted Nb (up to 250 nm in depth), decreasing to about 30 at.% for a thickness between 500 nm and 3.5  $\mu$ m in depth, by running HT-NPBII under similar conditions to the ones set in the current experiments.

The high temperature at which Nb was heated during nitrogen implantation led to the increase in size of the crystallites, as can be seen in Figures 5(b)–5(d), in comparison with the morphology of untreated Nb, as shown in Figure 5(a). It indicates the competition between the recovery and recrystallization processes, as a consequence of the reduction of the total area of the grain boundaries. In general, the creep mechanisms are affected by grain coarsening such as dislocation accommodated grain-boundary sliding (GBS)

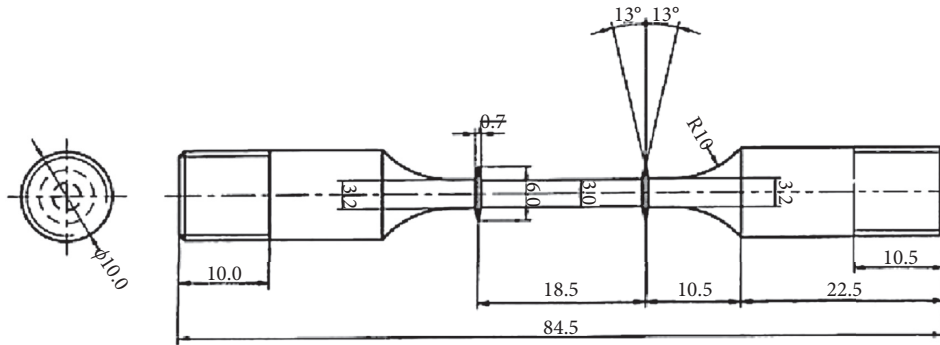


FIGURE 2: Schematic of the niobium specimen used for creep tests (dimensions in mm).

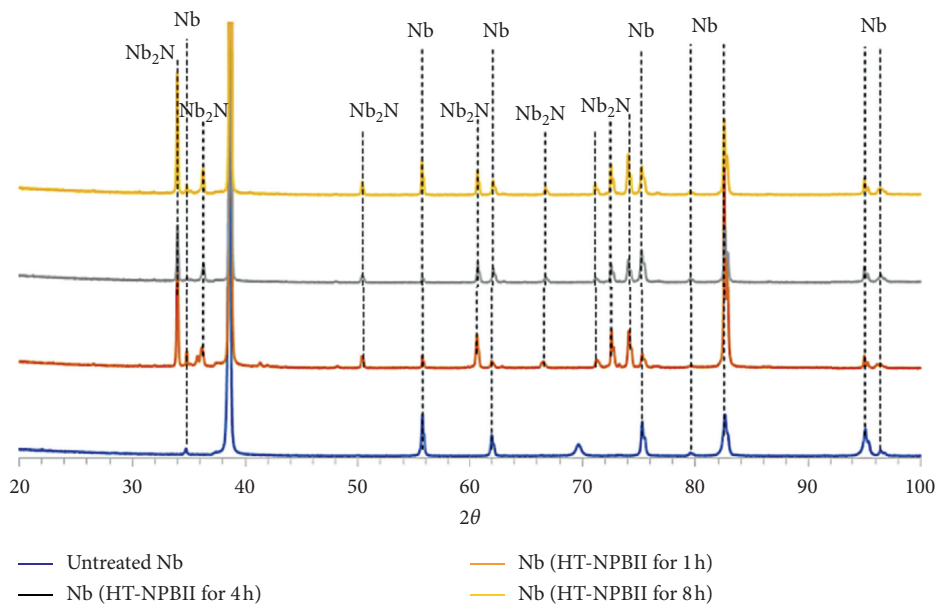


FIGURE 3: XRD for Nb samples treated by HT-NPBII at different experimental conditions in comparison with untreated Nb.

[18]. Thus, the increasing in grain size can improve the creep properties of the material once the total area of the grain boundaries is reduced, promoting increase in material resistance due to inhibit of sliding of dislocation during a mechanical loading.

The hardness of the treated specimens increased significantly compared to the untreated samples, as can be seen by the in-depth nanoindentation measurements presented in Table 1. A tenfold increase could be measured for indentation performed at  $3\ \mu\text{m}$  in depth, for a sample treated during 8 h. Decreasing values were measured for samples treated for 4 h and 1 h, respectively. The presence of refractory nitrides on the near surface of niobium, compounds that are as hard as ceramic materials, can explain the noticeable increase. On the contrary, the hardness measured in deeper layers (5, 10, 15, 20, and  $25\ \mu\text{m}$ ) remained higher than that achieved for untreated Nb, but with a two-fold increase only. This can be explained by the decrease in the atomic concentration of nitrogen implanted into Nb for the innermost metallic layers, preventing the formation of the respective nitrides, as previously reported by Oliveira et al. [3].

Treated and untreated Nb samples were submitted to creep tests performed under constants load and temperature

(35 MPa and  $500^\circ\text{C}$ ). The results, shown in Figure 6, exhibit a well-defined primary, secondary, and tertiary creep stages. As expected, a constant creep rate is observed at a larger period of creep life, associated to balance between the recovery and hardening process [13]. Table 2 summarizes the respective creep parameters, considering the primary creep time,  $t_p$ , secondary creep rate,  $\dot{\epsilon}'_s$ , and rupture time ( $t_f$ ). The reduction of the secondary creep rate for specimens treated for 1 h and 8 h, about one order of magnitude lower, in comparison with untreated Nb, can be observed. An atypical creep behavior was presented by the specimen treated for 4 h, without significant change of the secondary creep rate, although its rupture time was longer by considering other analyzed conditions. Similar fracture times were observed for specimens treated for 1 h and 4 h, with decrease in such values for specimens treated for 8 h. This unexpected behavior can be associated with the absorption of oxygen by the metal when treated for long time intervals. In fact, oxygen is an impurity hard to be removed from the walls of the vacuum chamber and even low atomic concentration levels of this element when attached to the metal can be detrimental leading to a decrease of the ductility of the

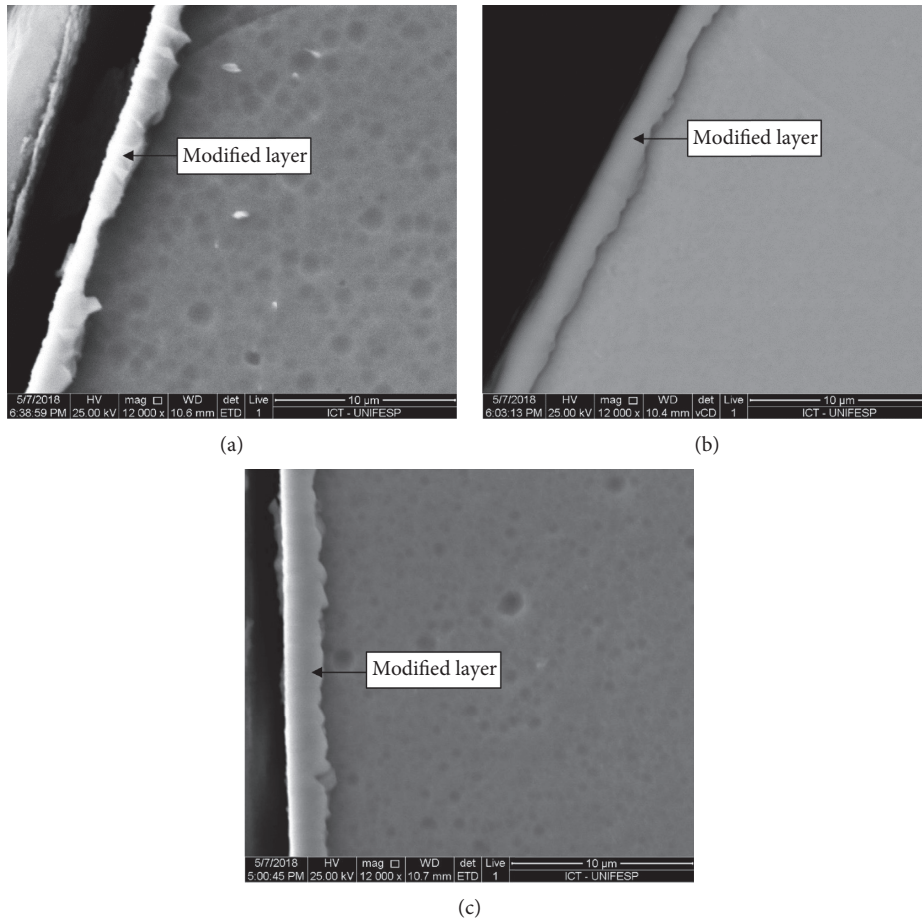


FIGURE 4: Cross-section view of treated niobium evidencing the modified layers after HT-NPBII performed at 1 h (a), 4 h (b), and 8 h (c).

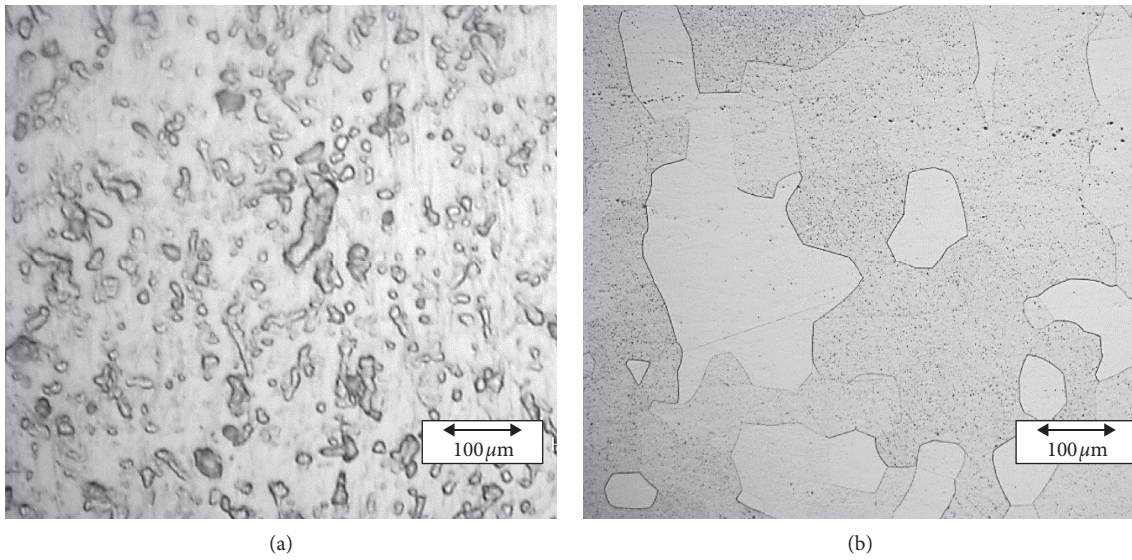


FIGURE 5: Continued.

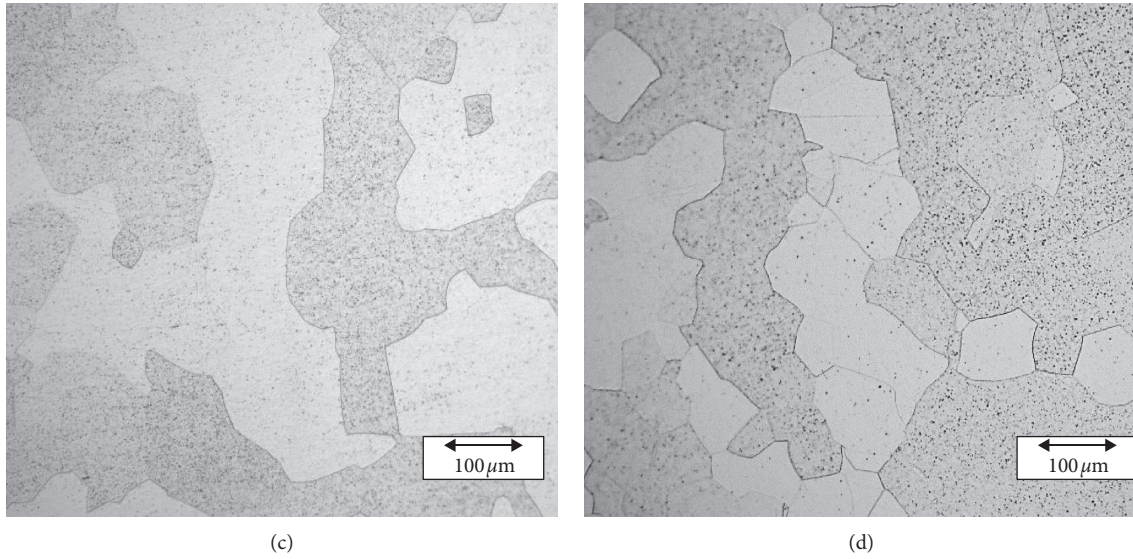


FIGURE 5: Comparison of the surface morphologies of untreated niobium (a), with samples submitted to HT-NPBII at treatment times of 1 h (b), 4 h (c), and 8 h (d), evidencing the enlargement of the grain sizes.

TABLE 1: Hardness distribution measured for treated and untreated samples in different regions of the material.

Depth ( $\mu\text{m}$ )	Average hardness (HV)			
	Untreated	HT-NPBII for 1 h	HT-NPBII for 4 h	HT-NPBII for 8 h
3	$247 \pm 15$	$1716 \pm 19$	$1926 \pm 29$	$2498 \pm 29$
5	$228 \pm 10$	$397 \pm 32$	$404 \pm 52$	$392 \pm 57$
10	$207 \pm 14$	$426 \pm 19$	$409 \pm 31$	$377 \pm 32$
15	$225 \pm 20$	$454 \pm 56$	$482 \pm 81$	$428 \pm 35$
20	$224 \pm 30$	$425 \pm 19$	$382 \pm 85$	$340 \pm 26$
25	$223 \pm 15$	$362 \pm 36$	$415 \pm 29$	$372 \pm 17$

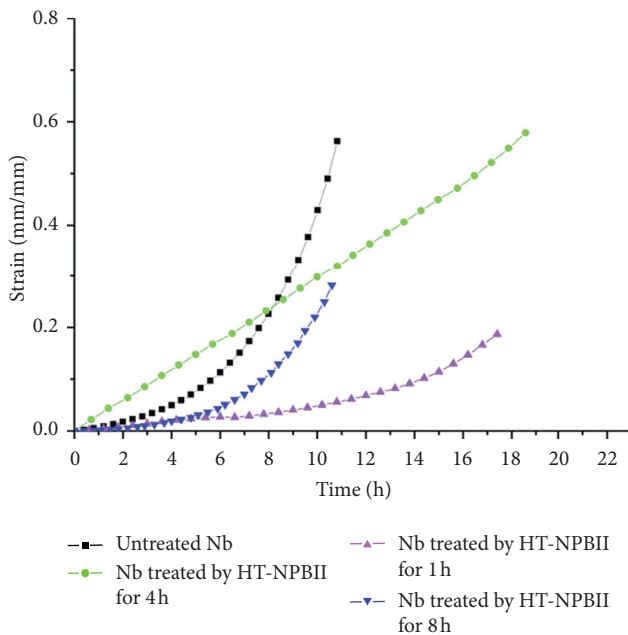


FIGURE 6: Typical creep curves of niobium treated by HT-NPBII submitted to creep tests at  $500^\circ\text{C}$  and 35 MPa.

specimen under mechanical loading. This problem can be mitigated through stringent vacuum conditioning procedures and is a hypothesis to be further verified.

Figure 7 shows results of additional creep tests of the niobium specimens treated for 1 h and performed under constant temperature ( $500^\circ\text{C}$ ) and different stress levels (25 MPa, 30 MPa, 35 MPa, and 40 MPa). Table 3 summarizes the respective creep parameters for these conditions, considering the primary creep time, secondary creep rate, and rupture time. The results show the influence of stress level variation in the creep behavior of the treated specimens, with a significant reduction in the secondary creep rate due to stress reduction employed during the creep test, of up to three orders of magnitude, varying from  $2.65 \times 10^{-2}$  1/h to  $5.10 \times 10^{-5}$  1/h for loads of 40 MPa and 25 MPa, respectively. According to Norton relation [13], this behavior is due to dependence between the imposed load with the material initial deformation and its creep rate, which increases for higher loads during the creep tests. Hence, the decrease of the stress level leads to the reduction of the secondary creep rate, improving the creep resistance of the material.

The results point out that the nitride layer acts as an effective barrier against oxygen diffusion into the material, improving its creep resistance. In fact, previous works have

TABLE 2: Creep data at 500°C and 35 MPa of untreated Nb and specimens treated by HT-NPBII for 1 h, 4 h, and 8 h.

Specimen	$t_p$ (h)	$\dot{\epsilon}'_s$ (1/h)	Strain (mm/mm)	$t_f$ (h)
Untreated	0.8	$11.12 \cdot 10^{-2}$	0.4291	10.1
HT-NPBII for 1 h	0.6	$5.25 \cdot 10^{-3}$	0.1870	17.4
HT-NPBII for 4 h	0.7	$2.96 \cdot 10^{-2}$	0.4955	18.5
HT-NPBII for 8 h	0.8	$9.63 \cdot 10^{-3}$	0.2820	10.6

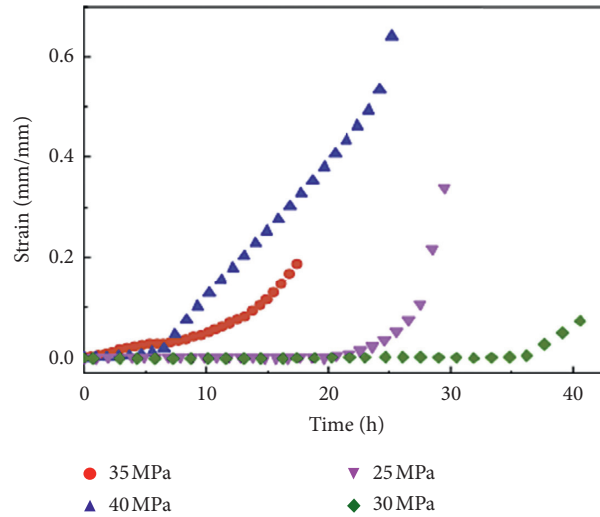


FIGURE 7: Typical creep curves of niobium treated by HT-NPBII for 1 h submitted to creep tests at 500°C and loads between 25 and 40 MPa.

TABLE 3: Creep data at 500°C and 35–40 MPa of niobium treated by HT-NPBII for 1 h.

$\sigma$ (MPa)	$t_p$ (h)	$\dot{\epsilon}_s$ ( $h^{-1}$ )	$\epsilon_f$ (mm/mm)	$t_f$ (h)
25	0.8	$5.10 \cdot 10^{-5}$	0.3382	29.5
30	0.6	$3.44 \cdot 10^{-5}$	0.0737	40.6
35	0.7	$5.25 \cdot 10^{-3}$	0.1870	17.4
40	0.8	$2.65 \cdot 10^{-2}$	0.8260	25.2

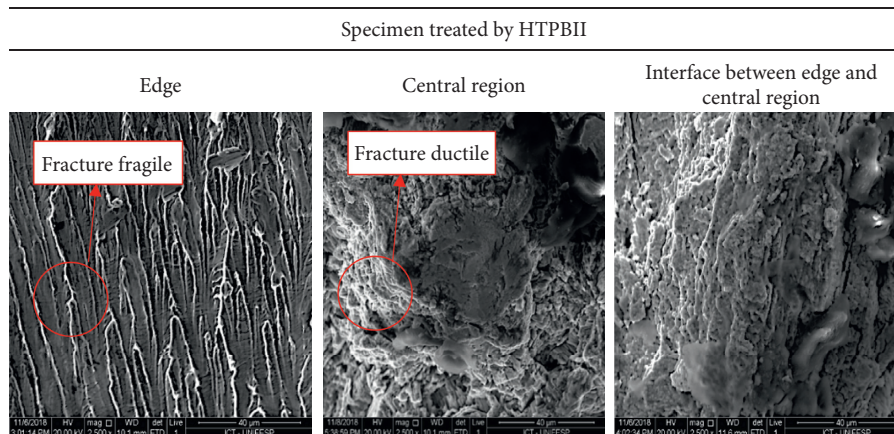


FIGURE 8: SEM micrograph of the fracture surface of a specimen treated for 1 h after creep tests at 500°C and 35 MPa.

demonstrated that a functional nitride surface can improve the performance of metallic materials at higher temperatures in the presence of the oxygen during creep resistance tests [4, 14, 15, 17].

The fracture surfaces' postcreep tests were analyzed by SEM, as shown in Figure 8. The results exhibit ductile fracture mechanisms with development of microcavities in the central region of the fractured specimens. In addition, a

fragile fracture behavior was observed at the edges of the treated samples, which seems to be associated with a lower ductility of the nitrides present in this region.

#### 4. Conclusions

HT-NPBII was effective for the formation of refractory niobium nitrides, leading to the improvement of the creep resistance of Nb for all of the heat treatment conditions analyzed. As specific conclusions,

- (i) The process led to the increase in size of grains of the substrate, affecting the creep mechanisms due to a reduction of the total area of the grain boundaries, which promotes an increase in material resistance due to inhibit of sliding of dislocation during a mechanical loading
- (ii) An increase in the hardness from about 247 HV up to about 2400 HV at longer treatment time, due to the presence of the refractory nitrides, was observed
- (iii) The effectiveness of HT-NPBII to produce a continuous layer of nitrides, acting as a diffusion barrier against inward oxygen diffusion on niobium surface and enhancing the creep resistance of the treated specimens, was observed
- (iv) The fractured surfaces' postcreep tests exhibited ductile fracture mechanism with development of microcavities in its central region, due to good niobium ductility, while a fragile fracture behavior was observed at the edge regions, associated in this case with the presence of niobium nitrides.

#### Data Availability

The data used to support the findings of the study are included within the article.

#### Conflicts of Interest

The authors declare that they have no conflicts of interest.

#### References

- [1] S. Gerardi and A. K. Suri, *International Metals Handbook*, ASM International, Materials Park, OH, USA, 10th edition, 1990.
- [2] T. Mukaibo, M. Kanno, and M. Yamawaki, "Oxidation behavior of Nb and Nb-V alloys," *Journal of Nuclear Science and Technology*, vol. 2, no. 12, pp. 516–524, 1965.
- [3] R. M. Oliveira, "Evaluation of the resistance to oxidation of niobium treated by high temperature nitrogen plasma based ion implantation," *Surface & Coatings Technology*, vol. 312, pp. 110–116, 2017.
- [4] A. C. Oliveira, R. M. Oliveira, D. A. P. Reis, and F. C. Carreri, "Effect of nitrogen high temperature plasma based ion implantation on the creep behavior of Ti-6Al-4V alloy," *Applied Surface Science*, vol. 311, pp. 239–244, 2014.
- [5] R. M. Oliveira, A. C. Oliveira, F. C. Carreri et al., "Detailed surface analyses and improved mechanical and tribological properties of niobium treated by high temperature nitrogen plasma based ion implantation," *Applied Surface Science*, vol. 283, pp. 382–388, 2013.
- [6] R. M. Oliveira, J. A. N. Gonçalves, M. Ueda, J. O. Rossi, and P. N. Rizzo, "A new high-temperature plasma immersion ion implantation system with electron heating," *Surface & Coatings Technology*, vol. 204, no. 18–19, pp. 3009–3012, 2010.
- [7] R. W. Evans and B. Wilshire, *Introduction to Creep*, The Institute of Materials, London, UK, 1993.
- [8] L. E. Toth, *Transition Metal Carbides and Nitrides*, Academic Press, New York, NY, USA, 1971.
- [9] R. M. Oliveira, C. B. Mello, G. Silva, J. A. N. Gonçalves, M. Ueda, and L. Pichon, "Improved properties of Ti6Al4V by means of nitrogen high temperature plasma based ion implantation," *Surface and Coatings Technology*, vol. 205, no. 2, pp. S111–S114, 2011.
- [10] F. C. Carreri, R. M. Oliveira, A. C. Oliveira et al., "Phase formation and mechanical/tribological modification induced by nitrogen high temperature plasma based ion implantation into molybdenum," *Applied Surface Science*, vol. 310, pp. 305–310, 2014.
- [11] J. Warren, L. M. Hsiung, and H. N. G. Wadley, "High temperature deformation behavior of physical vapor deposited Ti-6Al-4V," *Acta Metallurgica et Materialia*, vol. 43, no. 7, pp. 2773–2787, 1995.
- [12] P. Pérez, "Influence of nitriding on the oxidation behaviour of titanium alloys at 700°C," *Surface and Coatings Technology*, vol. 191, no. 2–3, pp. 293–302, 2005.
- [13] M. J. R. Barboza, C. Moura Neto, and C. R. M. Silva, "Creep mechanisms and physical modeling for Ti-6Al-4V," *Materials Science and Engineering: A*, vol. 369, no. 1–2, pp. 201–209, 2004.
- [14] A. G. d. Reis, D. A. P. Reis, C. de Moura Neto, M. J. R. Barboza, F. P. Neto, and J. Onôro, "Creep behavior study at 500°C of laser nitrided Ti-6Al-4V alloy," *Journal of Materials Research and Technology*, vol. 2, no. 1, pp. 48–51, 2013.
- [15] L. A. N. S. Reis, "The influence of laser nitriding on creep behavior of Ti-6Al-4V alloy with Widmanstätten microstructure," *Metals*, vol. 9, pp. 236–246, 2019.
- [16] M. Oliveira, L. M. Yogiaw, M. M. Silva et al., "Microstructural analysis of Ti-6Al-4V alloy after plasma immersion ion implantation (PIII)," *Materials Science Forum*, vol. 727–728, pp. 50–55, 2012.
- [17] *Annual Book of ASTM Standards in "American Society of Testing and Materials"*, Philadelphia, PA, USA, 1995.
- [18] A. Arieli and A. K. Mukherjee, "The rate-controlling deformation mechanisms in superplasticity—a critical assessment," *Metallurgical Transactions A*, vol. 13, no. 5, pp. 717–732, 1982.